



# Long time evolution of train dynamics with respect to track geometry

N. Lestoille, Christian Soize, G. Perrin, C. Fünfschilling

## ► To cite this version:

N. Lestoille, Christian Soize, G. Perrin, C. Fünfschilling. Long time evolution of train dynamics with respect to track geometry. The Second International Conference on Railway Technology: Research, Development and Maintenance (RAILWAYS 2014), Apr 2014, Ajaccio, France. pp.1-14. hal-00989424

**HAL Id: hal-00989424**

**<https://hal.science/hal-00989424>**

Submitted on 11 May 2014

**HAL** is a multi-disciplinary open access archive for the deposit and dissemination of scientific research documents, whether they are published or not. The documents may come from teaching and research institutions in France or abroad, or from public or private research centers.

L'archive ouverte pluridisciplinaire **HAL**, est destinée au dépôt et à la diffusion de documents scientifiques de niveau recherche, publiés ou non, émanant des établissements d'enseignement et de recherche français ou étrangers, des laboratoires publics ou privés.

# Long time evolution of train dynamics with respect to track geometry

N. Lestoille<sup>a,b</sup>, C. Soize<sup>a</sup>, G. Perrin<sup>a,b,c</sup>, C. Funfschilling<sup>b</sup>

<sup>a</sup>*Université Paris-Est, Laboratoire Modélisation et Simulation Multi Echelle, MSME UMR 8208 CNRS, 5 bd Descartes, 77454 Marne-la-Vallée, France.*

<sup>b</sup>*SNCF, Innovation and Research Department, Immeuble Lumière, 40 avenue des Terroirs de France, 75611 Paris, Cedex 12, France.*

<sup>c</sup>*Université Paris-Est, Laboratoire Navier (UMR 8205), CNRS, ENPC, IFFSTAR, 77454 Marne-la-Vallée, France.*

---

## Abstract

This paper aims at characterizing the long time evolution of the vehicle-track system. The knowledge of the evolution of such a system is of great concern for the railway industry, in order to maintain a high level of safety and comfort in the high speed trains. We propose a computational stochastic approach to predict the long time evolution of a given track portion. The approach is based on an adaptation of the global stochastic model of track irregularities previously identified with a large experimental data basis. The nonlinear stochastic dynamics of the train excited by track irregularities are carried out using a computational multibody dynamics model. Some indicators concerning the dynamic responses of the train are introduced in order to start off the maintenance or not of the given track portion.

*Key words:* high speed train dynamics, stochastic modeling, track irregularities, stochastic dynamics, long time evolution, vehicle-track coupling

---

## 1. Introduction

The tracks for high speed trains are submitted to more and more solicitations, because of the increase of the train traffic, the load and the speed of the trains. These solicitations induce degradations of the track geometry, making evolve track irregularities. Such degradations impact the train dynamic response in return. To guarantee a good level of safety and comfort of the train, maintenance operations of the track have to be regularly undertaken. These maintenance operations are heavy and costly. They would gain being started off by indicators on the train safety and comfort, and no

*In the proceedings of Railways 2014 Conference, Ajaccio, France, April 8-11, 2014.*

more on track-irregularities measures. However, the vehicle-track system is highly nonlinear and there is no obvious correlation between track irregularities and the vehicle-track forces (see [1, 2]). The knowledge of the effects of the track geometry on the train dynamic response needs to be increased in order to define robust indicators for the simulated train dynamic response and to characterize their evolution.

The goal of this study is to characterize the influence of the long time evolution of the track irregularities on the evolution of the train dynamic response. The distinction has to be done between the long time evolution, which will be denoted by  $\tau$ , and the time of the train dynamics (denoted by  $t$ ). Actually, the vehicle-track system is a complex system, with high nonlinearities and coupling between inputs (track geometry, track stiffness, track mass) and outputs (train responses). The track geometry is the main source of excitation for the train. The track geometry is known thanks to track measurements which are made very precisely and frequently. A global stochastic model of the track geometry has been built by Perrin *et al.* in [3] using a very large experimental data basis concerning the French railway network for high-speed trains. The stochastic modeling is very useful to carry out nonlinear stochastic dynamic analysis of the train excited by the random track geometry. Nevertheless, we need now to analyze the long time evolution of a given track portion, in order to construct criteria which allow maintenance operations to be started off. The most relevant information we have about the geometry of the given portion is only the projection of this portion on the global stochastic model. Since this projection requires a large number of coefficients (several thousands), the use of the long time evolution of all these coefficients does not allow to study the long time evolution of this portion, because the dimension (the number of coefficients) is too high. That is why we chose to analyze the long time evolution of the train dynamics on the given portion. For the long time evolution analysis of a given track portion, for which measurements are periodically carried out, the global stochastic model is adapted to this portion in introducing a noise which allows measurements errors and variability to be taken into account. Using this adapted stochastic model of the track geometry for such a given portion, the train dynamic response is numerically simulated using a commercial software (*Vampire*). To assess the long time evolution of the train dynamics, we have to define indicators on the train dynamic response and to observe their evolution over a long time.

Section 2 deals with the proposed approach. Section 3 will focus on the adapted stochastic modeling of the track irregularities, taking into account the measurements for the given track portion analyzed. In Section 4, the train dynamic response will be analyzed, setting up indicators on the train

dynamics to quantify the long time evolution of the train stability and comfort.

## 2. Proposed approach

### 2.1. Objectives

The track irregularities change during long time  $\tau$ , inducing modifications of the train dynamic response. Criteria of safety and comfort are needed to assess the long time evolution of the train dynamic response. To guarantee a good level of safety and comfort, maintenance operations on the track have to be regularly undertaken. The final objective of this work is to be able to decide to start off maintenance operations of a given track portion as a function of the simulated train dynamic response, and even to be able to anticipate maintenance operations. To achieve this goal, the long time evolution of the vehicle-track system has to be characterized using measurements of the track, which are periodically performed for the track portion under consideration.

The first main stage consists in studying the sensitivity of the train stochastic dynamics to the long time evolution of track irregularities.

### 2.2. Numerical simulation of the train dynamic response

The inputs of the simulation are the track design, the track irregularities modeled with the adapted stochastic model evoked in Section 1 and detailed in Section 3, and a model of the train. The model of the train used for the simulation is the one presented in [4]. It is a multibody dynamical system whose dynamic responses are computed using a commercial software (*Vampire*). It is assumed that the speed of the train is constant and fixed. The simulation outputs are accelerations in the train and contact forces between the wheels and the rails. The numerical simulation of the train response is performed on the given track portion for which the length,  $S$ , has to be defined.

The decision to start off the maintenance of the given portion is taken on the basis of indicators (called dynamic indicators) which are defined as functions of the train dynamic responses (outputs). These indicators must be sensitive to the long time evolution of the track irregularities. The dynamic indicators are based on statistical quantities related to the simulation outputs. Especially, random maxima of the stochastic outputs are of great concern, since we want to analyze safety and comfort levels for the given track portion. The obtained results could be used later to define thresholds on the dynamic indicators, in order to be able to start off maintenance operations from these thresholds.

It should be noted that, since the train is assumed to have a constant speed, it is equivalent to analyze the dynamic response as a function of the time  $t$  or as a function of the spatial location of the train defined by the curvilinear abscissa  $s$ . We also use the dual variable of  $s$  which is the wave number,  $k$ , and the associated wavelength  $\lambda = 2\pi/k$ . In such a case, we can use the terminology: “wavelength in the spectrum of the train dynamic response”.

### 2.3. Choice of the length of the studied given track portion

The length  $S$  of the given track portion has to be a compromise between the need of local information to start off the maintenance and the respect of characteristic lengths related to the train dynamics. Two characteristic lengths are taken into account to define  $S$ : the longest wavelength in the spectrum of the dynamic response and the length of the track transition section which is located between the given portion and the previous section used in the numerical simulation.

*Longest wavelength in the spectrum of the train dynamic response..* The train dynamic response is simulated on a section (including the given portion) which is much longer than the train length, to be sure to observe all the wavelengths contained in the spectrum of the train response. The power spectral density functions (spectrum) of the train responses are estimated (periodogram method with a Hamming window). Figure 1 displays an example for two outputs (vertical and lateral accelerations at a given location in the train). A length  $S_1$ , compatible with the shortest wave number,  $k_{\min}$

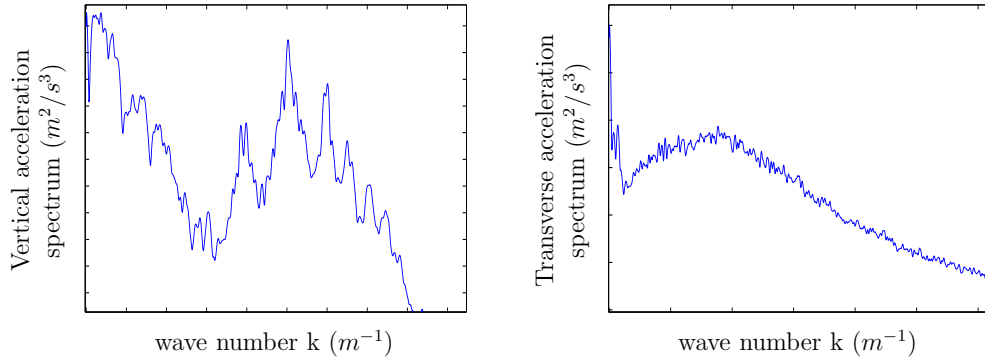


Figure 1: Power spectral density functions of two outputs of the simulated train dynamic response at a given location in the train.

is then defined such that:

$$S_1 \gg \frac{2\pi}{k_{\min}}. \quad (1)$$

*Length of the track transition section..* The length of the track transition section,  $S_{\text{trans}}$  is defined using 25 simulations of the train dynamics for 25 tracks made up of two successive portions including the same given portion. The length  $S_{\text{trans}}$  is such that the 25 train dynamic responses are the same on the portion  $S \setminus S_{\text{trans}}$ . Length  $S_2$  is chosen such that:

$$S_2 \gg S_{\text{trans}} . \quad (2)$$

*Length  $S$  of the studied given track portion..* Length  $S$  is defined as the maximum of  $S_1$  and  $S_2$ :

$$S = \max\{S_1, S_2\} . \quad (3)$$

### 3. Stochastic modeling of track irregularities

#### 3.1. Track measurements

The track geometry is measured by a measuring train very precisely and very frequently. The measuring train is equipped with laser cameras which measure the distances between the rails. The track is described by two data sets:

- the initial track design, which corresponds to the theoretical track (as it was planned before the construction) and which is made of perfect lines and curves.
- the irregularities of the track which appear during the track life cycle and which have to be added to the track design.

The track irregularities are modeled by a vector-valued random field  $\mathbf{X}$  denoted by

$$s \mapsto \mathbf{X}(s; \tau) = (X_1(s; \tau), X_2(s; \tau), X_3(s; \tau), X_4(s; \tau)) , \quad (4)$$

which is defined on  $S$  and which depends on long time parameter  $\tau$ . Its components are the lateral and vertical alignment irregularities  $X_1$  and  $X_2$ , the cant deficiencies  $X_3$  and the gauge irregularities  $X_4$ .

The given track portion is defined for  $s$  in  $\Omega = [0, S]$ , in which  $S$  the length chosen in Section 2.3. Long time  $\tau$  is a discrete parameter that rises between successive measurements of the given track portion,

$$\tau_0 < \tau_1 < \tau_2 < \dots < \tau_{\nu_\tau} , \quad (5)$$

in which  $\tau_0$  is the time of the first measurement just after a maintenance operation,  $\tau_1, \tau_2, \dots, \tau_{\nu_\tau}$  corresponds to the successive long times for which there are measurements of the track geometry, and  $\tau_{\nu_\tau}$  is the time of the last measurement before the next maintenance operation.

### 3.2. Adaptation of the global stochastic model of the track geometry to the given track portion

The global stochastic model proposed in [3] is very robust with respect to measurements errors. This model has the capability to generate a track irregularity for any given portion belonging to the French railway network. Nevertheless, as explained in Sections 1 and 2, we are interested in constructing a stochastic model adapted to the given track portion which has the capability to predict the long time evolution of this portion using the local measurements  $\mathbf{x}_{\tau_0}^{\text{meas}}, \mathbf{x}_{\tau_1}^{\text{meas}}, \mathbf{x}_{\tau_2}^{\text{meas}}, \dots$  of this portion at long times  $\tau_0, \tau_1, \tau_2, \dots$ . The objective of this adapted stochastic model which has to be constructed is (i) to take into account measurements noise associated with local measurements  $\mathbf{x}_{\tau_0}^{\text{meas}}, \mathbf{x}_{\tau_1}^{\text{meas}}, \mathbf{x}_{\tau_2}^{\text{meas}}, \dots$  and (ii) to take into account the local variability of the given track portion in order to decrease the “statistical distance” between the global stochastic model and the local measurements.

The method proposed to construct the adapted stochastic model of the track irregularities consists in introducing a random field noise for which the spatial properties are driven by the global stochastic model and whose intensity of its statistical fluctuations is identified at long time  $\tau_0$  using measurement  $\mathbf{x}_{\tau_0}^{\text{meas}}$ . This construction is detailed in Section 3.2.2. In order to simplify the reading, we give a short summary of the global stochastic modeling presented in [3] whose details can be found in [5, 6, 7, 8, 9].

#### 3.2.1. Short review on global stochastic modeling for track irregularities

The track irregularities vector  $\mathbf{X} = (X_1, X_2, X_3, X_4)$  is modeled by a vector-valued random field, defined on a probability space  $(\Theta, \mathcal{T}, \mathcal{P})$ , indexed by  $\Omega = [0, S]$ , with values in  $\mathbb{R}^4$ . It has been proven that random field  $\mathbf{X}$  is neither Gaussian nor stationnary (not homogeneous).

The global stochastic model of the track irregularities has been built and identified solving an inverse statistical problem using a very large experimental data basis related to the French railway network. Random field  $\mathbf{X}$  is centered,

$$E\{\mathbf{X}(s)\} = 0 \quad , \quad \forall s \in [0, S] , \quad (6)$$

where  $E\{\cdot\}$  is the mathematical expectation. The continuous vector-valued random field  $\mathbf{X}(s), s \in \Omega$ , is replaced by its spatial discretization at curvilinear abscissa  $s_n = nh$  with  $h$  the spatial step and  $n = 0, \dots, N_s$ , where  $S = N_s h$ . Keeping the same notation for the continuous random field and its spatial discretization, the following random vector is introduced,

$$\mathbf{X} = (\mathbf{X}(0), \mathbf{X}(h), \mathbf{X}(2h), \dots, \mathbf{X}(N_s h)) \quad (7)$$

with values in  $\mathbb{R}^{4(N_s+1)}$ .

The first step of the construction consists in using a truncated principal component representation of random vector  $\mathbf{X}$  which is written as

$$\mathbf{X} \simeq \sum_{k=1}^{N_\eta} \sqrt{\lambda_k} \mathbf{u}_k \eta_k, \quad (8)$$

in which  $N_\eta \ll 4(N_s + 1)$ , where  $\{\lambda_k, 1 \leq k \leq N_\eta\}$  are the  $N_\eta$  first largest eigenvalues, and where  $\{\mathbf{u}_k, 1 \leq k \leq N_\eta\}$  are the associated eigenfunctions of the covariance matrix  $[C_{\mathbf{X}\mathbf{X}}]$  of  $\mathbf{X}$ . The random coefficients  $\{\eta_k, 1 \leq k \leq N_\eta\}$  are non-correlated centered and normalized random variables such that:

$$\eta_k = \frac{1}{\sqrt{\lambda_k}} \mathbf{X}^T \mathbf{u}_k, \quad 1 \leq k \leq N_\eta. \quad (9)$$

Introducing the  $(4(N_s + 1) \times N_\eta)$  real matrix  $[U]$  defined by

$$[U] = [\mathbf{u}_1 \dots \mathbf{u}_{N_\eta}] \quad , \quad [U]^T [U] = [I], \quad (10)$$

in which  $[I]$  is the unity matrix, the diagonal matrix  $[\lambda]$  whose diagonal entries are  $\lambda_1, \dots, \lambda_{N_\eta}$ , and the random vector  $\boldsymbol{\eta}$  such that,

$$\boldsymbol{\eta} = (\eta_1, \dots, \eta_{N_\eta}), \quad (11)$$

then random vector  $\mathbf{X}$  can be rewritten as

$$\mathbf{X} \simeq [Q] \boldsymbol{\eta}, \quad (12)$$

in which the matrix  $[Q]$  is written as

$$[Q] = [\lambda]^{1/2} [U]. \quad (13)$$

The second step consists in constructing a polynomial chaos expansion [10, 11, 12] of the non-Gaussian second-order random vector  $\boldsymbol{\eta}$  whose non-correlated components are statistically dependent. The truncated polynomial chaos representation is then written as

$$\boldsymbol{\eta} \simeq \boldsymbol{\eta}^{\text{chaos}}(N) = \sum_{j=1}^N \mathbf{y}^{(j)} \psi_j(\boldsymbol{\xi}), \quad (14)$$

in which  $\boldsymbol{\xi} = (\xi_1, \dots, \xi_{N_g})$  is a uniform second-order centered random vector whose covariance matrix is the unity matrix (consequently, the components are statistically independent and have a unit variance). The non-Gaussian



dependent random variables  $\psi_1(\boldsymbol{\xi}), \dots, \psi_N(\boldsymbol{\xi})$  are the multivariate normalized Legendre polynomials of random vector  $\boldsymbol{\xi}$ . The parameters  $N_g$ ,  $N$  and  $N_\eta$  are identified in order to minimize the errors of approximation.

Using Equations (12) and (14), random vector  $\mathbf{X}$  can be represented by,

$$\mathbf{X} \simeq [Q] [y] \boldsymbol{\Psi}(\boldsymbol{\xi}), \quad (15)$$

in which the  $(N_\eta \times N)$  real matrix  $[y]$  is defined by  $[y] = [\mathbf{y}^{(1)} \dots \mathbf{y}^{(N)}]$  and where the  $\mathbb{R}^N$ -valued random variable  $\boldsymbol{\Psi}(\boldsymbol{\xi})$  is defined by  $\boldsymbol{\Psi}(\boldsymbol{\xi}) = (\psi_1(\boldsymbol{\xi}), \dots, \psi_N(\boldsymbol{\xi}))$ . Any realization  $\mathbf{X}(\theta)$ ,  $\theta \in \Theta$ , of random field  $\mathbf{X}$ , generated with the above stochastic model, is representative of the measurements  $\mathbf{x}_T^{\text{meas}}$ .

### 3.2.2. Local stochastic modeling

The local stochastic modeling consists in constructing an adapted stochastic model of the track irregularities related to a given track portion. Since the track irregularity is composed of four different and dependant types of irregularities, this model is adapted to each component  $X_1, X_2, X_3$  and  $X_4$  of the random field  $\{\mathbf{X}(s), s \in \Omega\}$ . The corresponding spatial discretization yields the following decomposition of the random vector  $\mathbf{X} = (\mathbf{X}^1, \mathbf{X}^2, \mathbf{X}^3, \mathbf{X}^4)$ . For  $k = 1, \dots, 4$ ,  $\mathbf{X}^k$  is a random vector of dimension  $N_s + 1$  which is rewritten (using Equation (12)) as

$$\mathbf{X}^k \simeq [Q^k] \boldsymbol{\eta}, \quad (16)$$

in which the  $((N_s + 1) \times N_\eta)$  real matrix  $[Q^k]$  is extracted from matrix  $[Q]$ . The proposed adapted stochastic model is written as

$$\tilde{\mathbf{X}}^k(\delta_k) = [Q^k] (\boldsymbol{\eta} + \delta_k \mathbf{G}^k), \quad k = 1, 2, 3, 4, \quad (17)$$

in which  $\boldsymbol{\delta} = (\delta_1, \delta_2, \delta_3, \delta_4)$  is the vector-valued parameter allowing the noise level to be controlled and which has to be identified using experimental data (see Section 3.2.3). For fixed  $k$ , the  $\mathbb{R}^{N_\eta}$ -valued random variable  $\mathbf{G}^k$  is a spatial discretization of a random field noise. In the model proposed,  $\mathbf{G} = (\mathbf{G}^1, \mathbf{G}^2, \mathbf{G}^3, \mathbf{G}^4)$  is chosen as a  $\mathbb{R}^{4N_\eta}$ -valued Gaussian second-order centered random variable whose covariance matrix is the unity matrix and which is defined on the probability space  $(\Theta', \mathcal{T}', \mathcal{P}')$ . From Equation (17), the adapted stochastic model can be rewritten as

$$\tilde{\mathbf{X}}^k(\delta_k) = \mathbf{X}^k + \mathbf{B}^k(\delta_k), \quad (18)$$

in which the random vector  $\mathbf{B}^k(\delta_k)$  which depends on  $\delta_k$  is such that

$$\mathbf{B}^k(\delta_k) = \delta_k [Q^k] \mathbf{G}^k. \quad (19)$$

### 3.2.3. Identification of the parameter $\delta^{\text{opt}}$

The optimal parameter  $\delta^{\text{opt}}$  is estimated by using the maximum log-likelihood method with experimental data. For fixed  $k$ , the following random observation is introduced,

$$W_k(\delta_k) = \frac{\|\tilde{\mathbf{X}}^k(\delta_k)\|}{E\{\|\mathbf{X}^k\|\}}. \quad (20)$$

in which  $\|\mathbf{X}^k\| = \|\tilde{\mathbf{X}}^k(0)\|$  is the Euclidean norm of the global stochastic model  $\mathbf{X}^k$ . We then introduce the random observation vector defined by

$$\mathbf{W}(\delta) = (W_1(\delta_1), W_2(\delta_2), W_3(\delta_3), W_4(\delta_4)). \quad (21)$$

For fixed  $k$ , the corresponding experimental measurement  $w_k^{\text{meas}}$  is defined by

$$w_k^{\text{meas}} = \frac{\|\mathbf{x}^{k,\text{meas}}\|}{E\{\|\mathbf{X}^k\|\}}, \quad 1 \leq k \leq 4. \quad (22)$$

Finally, the experimental observation vector  $\mathbf{w}^{\text{meas}}$  is introduced such that

$$\mathbf{w}^{\text{meas}}(\delta) = (w_1^{\text{meas}}(\delta_1), w_2^{\text{meas}}(\delta_2), w_3^{\text{meas}}(\delta_3), w_4^{\text{meas}}(\delta_4)). \quad (23)$$

Let  $\mathcal{L}_{\mathbf{W}}(\mathbf{w}^{\text{meas}}; \delta) = \log p_{\mathbf{W}}(\mathbf{w}^{\text{meas}}; \delta)$  be the log-likelihood in which  $p_{\mathbf{W}}(\mathbf{w}^{\text{meas}}; \delta)$  is the value of the probability density function  $\mathbf{w} \mapsto p_{\mathbf{W}}(\mathbf{w}; \delta)$  of random vector  $\mathbf{W}$  for  $\mathbf{w} = \mathbf{w}^{\text{meas}}$ . The optimal value  $\delta^{\text{opt}}$  is then identified solving the following optimization problem,

$$\delta^{\text{opt}} = \arg \max_{\delta} \{\mathcal{L}_{\mathbf{W}}(\mathbf{w}^{\text{meas}}; \delta)\}. \quad (24)$$

The quantity  $p_{\mathbf{W}}(\mathbf{w}^{\text{meas}}; \delta)$  is computed using independent realizations of  $\mathbf{W}$  generated with the adapted stochastic model and fitted by using the multivariate Gaussian kernel method (see for instance [13, 14]).

### 3.2.4. Adapted stochastic modeling for the long time evolution of a given track portion

For a given track portion, it is assumed that  $\nu_{\tau}+1$  measurements  $\mathbf{x}_{\tau_0}^{\text{meas}}, \dots, \mathbf{x}_{\tau_{\nu_{\tau}}}^{\text{meas}}$  corresponding to long times  $\tau \in \{\tau_1, \dots, \tau_{\nu_{\tau}}\}$  are available. The optimal value  $\delta^{\text{opt}}$  of  $\delta$  is identified using only time  $\tau_0$  (the first time).

$$\delta^{\text{opt}} = \arg \max_{\delta} \{\mathcal{L}_{\mathbf{W}}(\mathbf{w}_{\tau_0}^{\text{meas}}, \delta)\}. \quad (25)$$

It is then assumed that this optimal value is representative to construct the adapted stochastic modeling allowing the long time evolution of this given track portion to be estimated.

The admissible set for  $\boldsymbol{\delta}$  is defined as the domain  $[0, 2]^4$  of  $\mathbb{R}^4$ . For estimating the optimal value, the following deterministic search algorithm is used. The identification of  $\boldsymbol{\delta}^{\text{opt}}$  is made in two steps. The admissible set is partitioned in  $20^4$  meshes corresponding to a constant step of 0.1 for each coordinate. For each value of  $\boldsymbol{\delta}$  corresponding to a node of the mesh, the log-likelihood is computed with 10,000 realizations of  $\mathbf{W}(\boldsymbol{\delta})$ . This stage allows the node of the mesh corresponding to the maximum of the log-likelihood to be identified and this node is then denoted as  $\boldsymbol{\delta}^1 = (\delta_1^1, \delta_2^1, \delta_3^1, \delta_4^1)$ . Since the dimension of the admissible set of parameter  $\boldsymbol{\delta}$  is small, and since each component  $\delta_k$  belongs to a given finite interval, a deterministic algorithm can be used for solving the optimization problem defined by Equation (25). Then, the subdomain  $\Pi_{k=1}^4 [\delta_k^1 - 0.25, \delta_k^1 + 0.25]$  is explored for  $\boldsymbol{\delta}$  with a precision of 0.05 for each coordinate ( $10^4$  meshes for the subdomain). The log-likelihood is computed with 100,000 realizations for  $\mathbf{W}(\boldsymbol{\delta})$ . Figure 2 displays the sections (following each coordinate  $\delta_k$  of  $\boldsymbol{\delta}$ ) of the hypersurface defined by the graph  $\boldsymbol{\delta} \mapsto \mathcal{L}_{\mathbf{W}}(\mathbf{w}_{\tau_0}^{\text{meas}}, \boldsymbol{\delta})$  of the multidimensional log-likelihood function. For this given track portion, the estimated optimal value  $\boldsymbol{\delta}^{\text{opt}}$  is

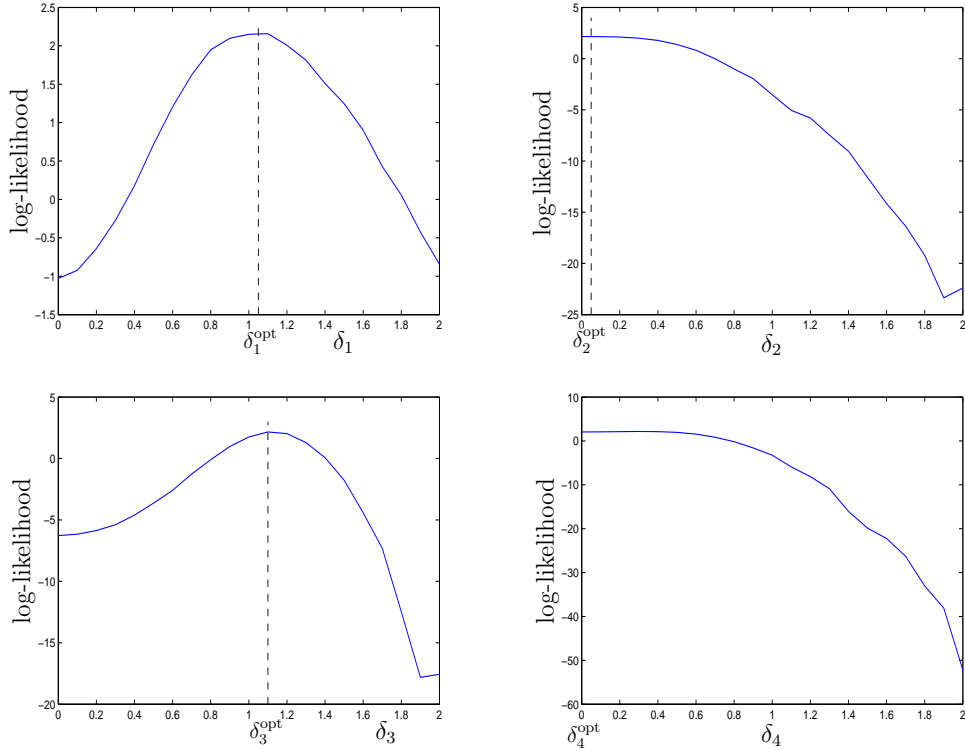


Figure 2: Sections of the log-likelihood  $\mathcal{L}_{\mathbf{W}}(\mathbf{w}_{\tau_0}^{\text{meas}}, \boldsymbol{\delta})$  for each component  $\delta_k$  of  $\boldsymbol{\delta}$

$$\boldsymbol{\delta}^{\text{opt}} = (1.05, 0.05, 1.1, 0). \quad (26)$$

The values obtained for each coordinate are coherent with Figure 2. The variation of the marginal probability density function (PDF)  $w_1 \mapsto p_{W_1(\delta_1)}(w_1; \delta_1)$  of random variable  $W_1(\delta_1)$  is plotted in Figure 3 as a function of  $\delta_1$ .

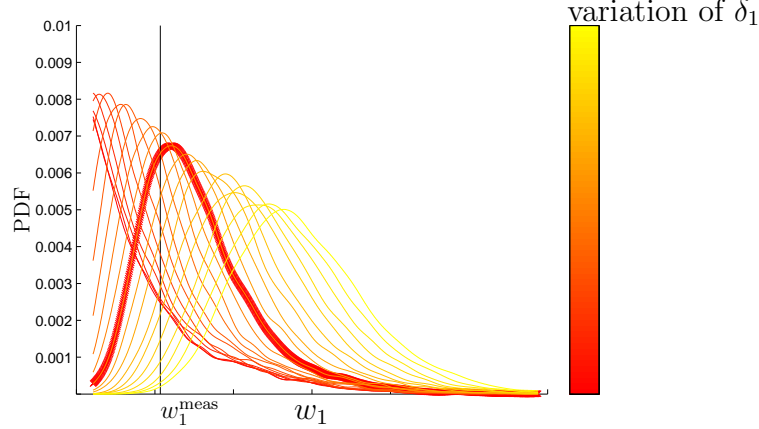


Figure 3: Graphs the PDF,  $w_1 \mapsto p_{W_1(\delta_1)}(w_1; \delta_1)$ , in function of  $\delta_1$  (the bold line is obtained for  $\delta_1 = \delta_{1,\text{opt}}$ ).

The adapted stochastic modeling of the long time evolution for the given track portion is constructed as follows. At long time  $\tau$ , the measurement  $x_\tau^{\text{meas}}$  is projected on the global stochastic model defined by Equation (12). Taking into account Equations (10) and (13) yields the projection  $\boldsymbol{\eta}_\tau^{\text{meas}}$  which is written as

$$\boldsymbol{\eta}_\tau^{\text{meas}} = [\mathbf{Q}]^T [\boldsymbol{\lambda}]^{-1} (\mathbf{x}_\tau^{\text{meas}}). \quad (27)$$

Then, this projection is used in the adapted stochastic model defined by Equation (17) and gives

$$\tilde{\mathbf{X}}_\tau^k(\delta_k^{\text{opt}}) = [\mathbf{Q}^k] (\boldsymbol{\eta}_\tau^{\text{meas}} + \delta_k^{\text{opt}} \mathbf{G}^k) \quad , \quad k = 1, 2, 3, 4. \quad (28)$$

As an illustration,  $\mathbf{x}_{\tau_0}^{1,\text{meas}}$  and the confidence region at 95% of  $\tilde{\mathbf{X}}_{\tau_0}^1(\delta_1^{\text{opt}})$  are compared in Figure 4. It can be noticed that the geometrical and physical properties of the irregularities are preserved with the identified adapted stochastic modeling.

## 4. Dynamic response of the train

### 4.1. Stochastic dynamic response of the train

For fixed long time  $\tau$ , the stochastic model of the track irregularities is given by  $\tilde{\mathbf{X}}_\tau^k(\delta_k^{\text{opt}})$ ,  $k = 1, 2, 3, 4$ , defined by Equation (28). The stochastic

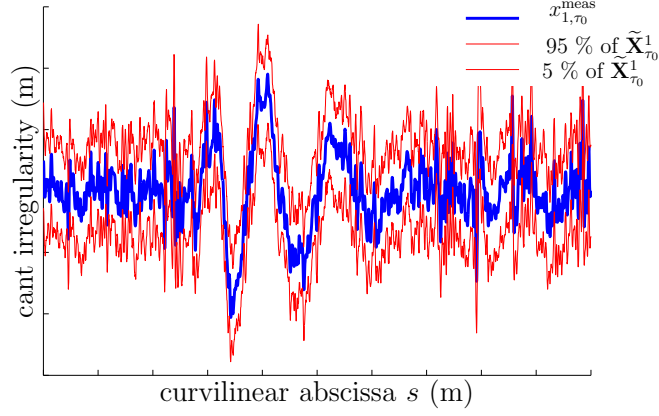


Figure 4: Irregularity  $x_{\tau_0}^{1,\text{meas}}$  and confidence region at 95% of  $\tilde{\mathbf{X}}_{\tau_0}^1(\delta_1^{\text{opt}})$  for the given track portion.

response of the train is then computed using the Monte-Carlo method. For each realization  $\tilde{\mathbf{X}}_{\tau}^k(\delta_k^{\text{opt}}; \theta')$  for  $\theta' \in \Theta'$ , the deterministic realization of the train response is computed. The set of these realizations allows statistical estimators to be constructed for analyzing the stochastic responses through dynamic indicators. The calculations are performed with 100 realizations and the responses are expressed in terms of the curvilinear abscissa  $s = vt$ , in which  $v$  is the constant speed of the train and  $t$  is the time of the train dynamics. The train is a TGV Duplex for which the number of wheelsets is  $\nu_w = 26$ , and wheelsets are numbered  $j = 1, \dots, \nu_w$ .

#### 4.2. Description of the dynamic indicators

The chosen dynamic indicators are based on criteria described in norm UIC 518 [15] for the homologation of railway vehicles. These indicators  $C_j^k$  are related to each wheelset,  $j$ , and are functions of the dynamic outputs  $A_j^k(s)$  which are themselves functions of index  $R$  which stands for “right wheel” and of index  $L$  which stands for “left wheel”, and of curvilinear abscissa  $s$ . The dynamic outputs are:

- the sum of the lateral forces on each wheelset,  $A_j^1 = (Y_{j,R} + Y_{j,L})(s)$ ;
- the maximum between right and left wheels of the quotient of transverse forces  $Y$  on vertical load  $Q$  at wheel-rail contact, which is defined by the quantity  $A_j^2 = \max\{(Y_{j,R}/Q_{j,R})(s), (Y_{j,L}/Q_{j,L})(s)\}$ ;
- the lateral accelerations,  $A_j^3 = \ddot{Y}_j(s)$ ;

- the vertical accelerations,  $A_j^4 = \ddot{Z}_j(s)$ ;
- the sum of the right and the left vertical forces on each wheelset,  $A_j^5 = (Q_{j,R} + Q_{j,L})(s)$ ;
- the difference between the right and the left vertical forces on each wheelset,  $A_j^6 = (Q_{j,R} - Q_{j,L})(s)$ .

According to [15], these indicators are smoothed and filtered. The indicator  $C_j^k$  is defined by

$$C_j^k = \max_{s \in [0, S]} |A_j^k(s)| \quad , \quad 1 \leq j \leq \nu_w \quad , \quad 1 \leq k \leq 6. \quad (29)$$

The number of indicators is reduced with respect to the number of wheelsets in analyzing the correlation between them. The indicators which are strongly correlated are removed. For instance, the correlation matrix for the sum of lateral forces restricted to 15 wheelsets among the 26 is plotted in Figure 5. Finally, 7 indicators on 6 wheelsets are kept, which yields 42 indicators to assess the train dynamic response.

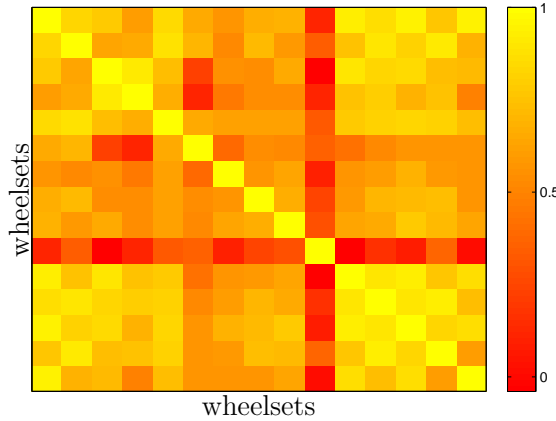


Figure 5: Correlation between the indicators on the sum of lateral forces for 15 wheelsets.

#### 4.3. Long time evolution of the dynamic indicators

We are now able to assess the train dynamic response on a given track portion and to observe its long time evolution as a function of  $\tau$  using the dynamic indicators  $C_i^k(\tau)$ ,  $1 \leq i \leq 6$ ,  $1 \leq k \leq 7$ . For each time  $\tau$ , the probability density function (PDF) of  $C_i^k(\tau)$  is plotted in Figure 6. Its long time evolution shows an increase and a dispersion of the safety and comfort indicators of the train dynamics.

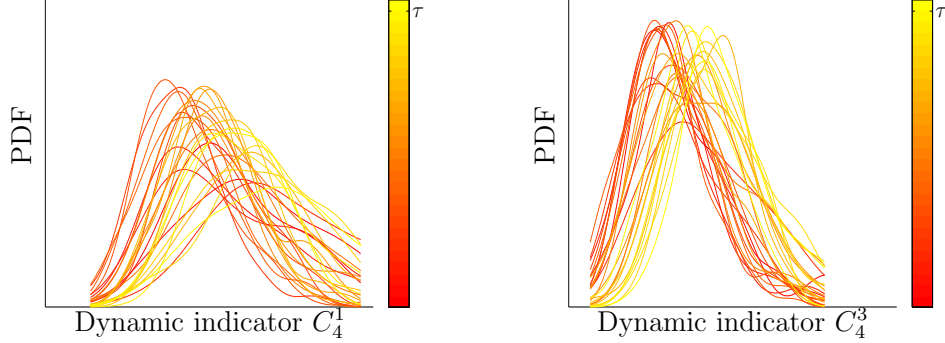


Figure 6: Evolution of the PDF of the dynamic indicators  $C_4^1$  and  $C_4^3$  as a function of time  $\tau$ .

## 5. Conclusion and perspectives

This work corresponds to a first step of the development of a stochastic modeling allowing the long time evolution of a given track portion to be analyzed. The stochastic model which is proposed has been constructed using a very large experimental data basis related to all the french railway network for the high speed trains, and consequently, can be considered as very robust. The next steps which are in progress consist in introducing uncertainties in the dynamical model of the train and in developing a stochastic model for the long time evolution.

## Acknowledgement

This work was supported by SNCF.

## References

- [1] M. X. D. Li, E. G. Berggren, M. Berg and I. Persson, “Assessing track geometry quality based on wavelength spectra and track-vehicle dynamic interaction”, *Vehicle System Dynamics*, 46, 261-276, 2008.
- [2] G. Lonnbark, “Characterization of track irregularities with respect to vehicle response” Technical Report, TRITA AVE 2012:30, Royal Institute of Technology, Stockholm, Sweden, 2012.
- [3] G. Perrin, C. Soize, D. Duhamel, C. Funfschilling, “Track irregularities stochastic modeling”, *Probabilistic Engineering Mechanics*, 34, 123-130, 2013.
- [4] S. Kraft, “Parameter identification for a TGV model”, *Thèse de Doctorat*, Ecole Centrale Paris, France, 2012.

- [5] G. Perrin, “Random fields and associated statistical inverse problems for uncertainty quantifications - Applications to railway track geometries for high-speed trains dynamical responses and risk assessment”, Thèse de Doctorat, Université Paris-Est, France, 2013.
- [6] G. Perrin, C. Soize, D. Duhamel, C. Funfschilling, “Identification of polynomial chaos representations in high dimension from a set of realizations” SIAM Journal of Scientific Computing, 34(6), A2917-A2945, 2012.
- [7] C. Soize, “Identification of high-dimension polynomial chaos expansions with random coefficients for non-Gaussian tensor-valued random fields using partial and limited experimental data”, Computer Methods in Applied Mechanics and Engineering, 199, 2150-2164, 2010.
- [8] G. Perrin, C. Soize, D. Duhamel, C. Funfschilling, “Karhunen-Love expansion revisited for vector-valued random fields: scaling, errors and optimal basis”, Journal of Computational Physics, 242(1), 607-622, 2013.
- [9] G. Perrin, C. Soize, D. Duhamel, C. Funfschilling, “A posteriori error and optimal reduced basis for stochastic processes defined by a finite set of realizations”, SIAM/ASA, Journal of Uncertainty Quantification, *submitted*, 2013.
- [10] R. Ghanem, P. Spanos, “Stochastic finite elements: a spectral approach”, Dover Publications, New York, 2003 (1st edition: Springer-Verlag, New York, 1991).
- [11] O. Le Maitre, O. Knio, “Spectral Methods for Uncertainty Quantification” Springer, 2010.
- [12] C. Soize, “Stochastic Models of Uncertainties in Computational Mechanics”, ASCE, Reston, VA, USA, 2012.
- [13] G. R. Terrell, D. W. Scott, “Variable Kernel Density Estimation”, The Annals of Statistics, 20(3), 1236-1265, 1992.
- [14] A. W. Bowman and W. Azzalini, “Applied Smoothing Techniques for Data Analysis”, Oxford University Press, Oxford, 1997.
- [15] UIC, “Testing and approval of railway vehicles from the point of view of their dynamic behaviour - Safety - Track fatigue - Running behaviour” UIC Leaflet 518, Paris, France, 2009.